Exciton states in coupled double quantum wells in a static electric field

M. M. Dignam and J. E. Sipe
Department of Physics and Ontario Laser and Lightwave Research Centre, University of Toronto, Toronto, Ontario, Canada M5S 1A7
(Received 27 June 1990; revised manuscript received 10 September 1990)

We calculate variationally the four lowest energy levels and oscillator strengths of 1*s* excitons in a coupled-double-quantum-well structure in an applied static electric field. We demonstrate the importance of employing a variational wave function, which allows for single-particle-state mixing, and which treats the in-plane radial dependence of the exciton states in a more sophisticated manner than the commonly used single exponential. We accomplish this by expanding the eigenstates in a basis consisting of *exciton* wave functions rather than the commonly used basis of *free* electron and hole wave functions. These basis wave functions are the ground states of the excitonic Hamiltonians where the electron is primarily confined to one layer and the hole to another—possibly the same—layer. We apply this method to symmetric coupled wells as well as to an asymmetric structure in which the electron and hole in the ground state are localized in separate layers even in the absence of an applied electric field. From an analysis of our results, we arrive at a general approach to qualitatively understand and classify the excitonic properties of these structures.

I. INTRODUCTION

The investigation of excitons in quantum wells, coupled double quantum wells, and superlattices has been an area of intense study for the past decade. Particular attention has been paid to the effect of a static electric field applied parallel to the structure growth axis. The interest in these structures is due both to their importance in understanding the fundamental processes in quantum structures and to their applications in electro-optic devices.[1–3] Although there has been a considerable amount of experimental work done on the exciton states in these structures,[4–10] almost all the theoretical work done to date has concentrated on quantum wells,[11] with only a few calculations made for the more complicated coupled-double-well[10,12–14] or superlattice[15–19] structures.

In the case of the single quantum well, it has been found that an accurate variational wave function for the exciton ground state can be written as the product of three functions: a function depending only on the radial (in-plane) distance between the electron and hole, the single-particle electron ground-state wave function, and the single-particle hole ground-state wave function.[11] It is generally found that the inclusion of the excited single-particle states in the variational wave function leads to a negligible improvement in the results because, except in the case of very narrow or very wide well widths, the energy separation of these levels from the single-particle ground state is very large (~ 100 meV) relative to the Coulomb energy (~ 10 meV). In a superlattice (SL) or a coupled-double-quantum-well (CDQW) structure, this energy separation can be much less, and so mixing via electron-hole Coulomb interaction can become important. Although this mixing has always been taken into account in SL exciton calculations,[15–19] where the levels form a continuum, its importance has not always been fully recognized in the case of a CDQW,[10,14] even though in wide barrier structures the level separation can be much less than 1 meV.

Perhaps even more importantly, it has not been generally recognized that the excitons in CDQW's (and SL's) have a true three-dimensional character, and hence one cannot accurately approximate their wave functions as a separable product, in the way that one can for exciton wave functions in a single quantum well. A common approach has been to write the CDQW (or SL) exciton wave function as a product of a sum of single-particle electron wave functions with a sum of single-particle hole wave functions, and to multiply these by a single exponential of radial dependence.[13,16,17] We find that this can lead to a serious underestimation of the binding energies in CDQW's, *particularly when a static electric field is applied.* In fact, the calculation of Galbraith and Duggan[13] predicts the existence of a blue shift of the ground state for small applied electric fields—a shift that, in light of our calculations, appears to be the artifact of an insufficiently flexible variational wave function.

Finally, many of the calculational methods that have been used to date[10,13,16,17] calculate only the excitonic ground state in CDQW and SL structures. However, in the presence of an applied static electric field, the states of excited along-axis motion have profound effects on the absorption spectra, both in superlattices[20–25] (Stark ladder) and CDQW's.[5–9] Even in the absence of an electric field, the oscillator strength of the higher states can be non-negligible.[5,15] It is therefore clear that if one is to understand the experimentally obtained spectra, it is essential that the method of calculation describe some of the excited states as well as the ground state.

In a previous publication we presented the results of a calculation of exciton states in a *superlattice* in an applied

electric field[20] which exhibited good agreement with the experimentally obtained Stark ladder spectrum.[22] In this paper we adapt this approach to the case of a CDQW structure in an applied static electric field. In essence, we solve for the 1s exciton states by diagonalizing the Hamiltonian in a restricted basis of "two-well" 1s exciton wave functions, rather than the more commonly used basis of single-particle eigenstates. Such an approach captures the essential three-dimensional characteristics of the wave function, takes the coupling of the single-particle states into account, and leads naturally to the calculation of the first four 1s-like exciton states. In addition, the method is relatively simple in concept and implementation. From our results and via a comparison with the results of others, we feel that this work captures most of the important qualitative *and* quantitative features of exciton states in CDQW's.

In Sec. II of this paper we present our method of calculation for exciton states in CDQW structures in the presence of an applied static electric field. In Sec. III we present the results and discussion for different $GaAs/Ga_{1-x}Al_xAs$ symmetric structures as a function of barrier width in the absence of an applied electric field, and compare our results with the theoretical results of previous authors. In Sec. IV we present our results for the electric field dependence of the energies and absorption strengths for the four lowest 1s exciton states in several symmetric structures; we compare our results with the experimental data of Chen *et al.*,[5] and find good agreement. In Sec. V we present the results for an asymmetric two-well structure in which the excitonic ground state exhibits a large dipole moment even before an electric field is applied. Finally, in Sec. VI we summarize our results and comment on their importance in understanding these structures.

II. THEORY

The Hamiltonian for the exciton envelope function in a CDQW with the growth axis in the z direction may be written[15]

$$\begin{aligned} H(z_e,z_h,r)=&H_0(z_e,z_h,r)+V_1^e(z_e-s_1)\\ &+V_2^e(z_e-s_2)+V_1^h(z_h-s_1)\\ &+V_2^h(z_h-s_2)+eFz\ , \end{aligned} \tag{2.1}$$

where H_0 contains the kinetic and Coulomb energy terms,

$$\begin{aligned} H_0(z_e,z_h,r)=&-\frac{\hbar^2}{2\mu(z_e,z_h)}\frac{1}{r}\frac{\partial}{\partial r}\left[r\frac{\partial}{\partial r}\right]\\ &-\frac{\hbar^2}{2}\frac{\partial}{\partial z_e}\frac{1}{m_{ez}^*(z_e)}\frac{\partial}{\partial z_e}\\ &-\frac{\hbar^2}{2}\frac{\partial}{\partial z_h}\frac{1}{m_{hz}^*(z_h)}\frac{\partial}{\partial z_h}\\ &-\frac{e^2}{\epsilon(r^2+z^2)^{1/2}}\ , \end{aligned} \tag{2.2}$$

and where $V_i^e(z)$ $[V_i^h(z)]$ is the potential for the ith well for the electron (hole):

$$V_i^\sigma(z)=\begin{cases}-v_i^\sigma & \text{if } |z|<L_i/2,\\ 0 & \text{otherwise.}\end{cases} \tag{2.3}$$

Here, $\sigma=\{e,h\}$, denoting an electron or a hole, L_i is the width of the ith well ($i=\{1,2\}$), and v_i^e (v_i^h) is the conduction- (valence-) band discontinuity between the barrier material and the material in the ith well (see Fig. 1). We have taken the origin for both the electron and hole coordinates to be the center of the barrier, while $s_1=-(L_b+L_1)/2$ and $s_2=(L_b+L_2)/2$ give the coordinates of the centers of the two wells, where L_b is the barrier width. The positions of the electron and hole are specified by their z coordinates z_e and z_h, respectively ($z\equiv z_e-z_h$), by the projection r of the distance between them onto the xy (transverse) plane, and by the x and y coordinates of their center of mass. The last two variables, as well as the momentum of the center of mass of the exciton, describe the free motion of the exciton in the plane; the corresponding part of the Hamiltonian is separable from the part appearing in Eq. (2.2). The layer-dependent transverse electron-hole reduced effective mass is denoted by $\mu(z_e,z_h)$, and the layer-dependent effective masses of the electron and hole in the z direction are denoted by $m_{ez}^*(z_e)$ and $m_{hz}^*(z_h)$, respectively. Finally, F is the applied static electric field and ϵ is an average static dielectric constant of the structure.

In choosing the above Hamiltonian, we have ignored valence-band mixing and band nonparabolicity, but have taken into account the differences in the effective masses in the two materials. In light of previous work[15,20] we feel that the effects of these neglected factors can be largely incorporated by an appropriate choice of effective masses. Further, they are not particularly important for achieving an understanding of the essential features of the 1s excitons of these structures. Admittedly, they change the calculated energies and absorption strengths by relatively small but non-negligible amounts,[18,24] and will account for small anticrossings between the light- and heavy-hole exciton levels as a function of the electric field strength.[5] The approach of this paper could be generalized to allow for a Hamiltonian more accurate than that of Eq. (2.1), which would take these factors into ac-

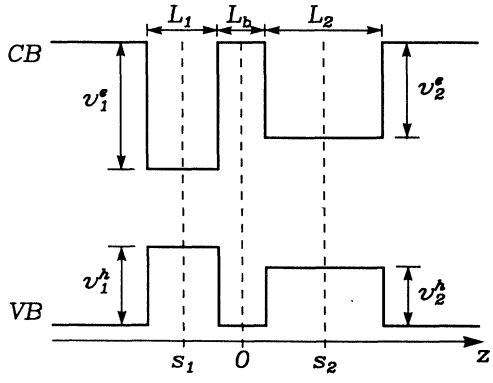

FIG. 1. The conduction- and valence-band edges as a function of z for the general coupled-double-well structure. In all sections other than Sec. V, we take $L_1=L_2$ and $v_1^\sigma=v_2^\sigma$.

count.

We employ a variational approach to find the energies and oscillator strengths in a CDQW. Our variational approach differs from those used by others[10,12–14] in two important respects. First, we use a basis set that is appropriate for determining not only the *ground* 1*s* exciton state, but the excited 1*s* exciton states as well. This is important, especially for the problem of a CDQW in a static electric field, since the excited states can have much larger oscillator strengths than the ground state, and are thus the experimentally accessible states. Second, we use a basis set that is flexible enough to treat separately the r dependence of the physically distinct parts of the exciton wave function, namely the parts in which the electron and hole are in the *same* well and the parts in which they are in *different* wells. We find below that this is crucial in constructing wave functions to accurately estimate binding energies, because the Coulomb interaction is effectively much larger when the electron and hole are in the same well than when they are in different wells.

It is primarily the identification of such a basis, which is simple to construct and easy to employ in realistic calculations, that distinguishes our method from those of previous workers. The basis set consists of the ground states of the electric-field-dependent two-well Hamiltonians,

$$\mathcal{H}_{ij}=H_0(z_e,z_h,r)+U_i^e(z_e-s_i)+U_j^h(z_h-s_j)\ , \tag{2.4}$$

where

$$U_i^\sigma(z_\sigma-s_i)\equiv V_i^\sigma(z_\sigma-s_i)-q_\sigma FQ_i^\sigma(z_\sigma-s_i) \tag{2.5}$$

and

$$Q_i^\sigma(z)=\begin{cases}-L_i/2 & \text{if } z<-L_i/2,\\ z & \text{if } |z|\le L_i/2,\\ L_i/2 & \text{if } z>L_i/2,\end{cases} \tag{2.6}$$

and $q_e=-|e|$ and $q_h=|e|$. In the absence of an electric field, these are just the *excitonic* Hamiltonians in which the electron sees the potential due to only *one* of the quantum wells (the ith) and in which the hole sees the potential due to another single well (the jth) that may or may not be associated with the same layer. In the presence of an electric field, the second term on the right-hand side of Eq. (2.5) takes into account the essential aspects of the quantum confined Stark effect[25,26] (QCSE) for a particle in a single well (see Fig. 2). In including the overall bias setup across the well, as well as the variation of the potential within, this term describes the part of the potential due to the presence of the electric field *in* the well. The ground states of $\mathcal{H}_{ij}$ thus reflect the presence of this field, which is a matter of importance in Sec. IV.

We now note that for any of the four sets of pairs (ij), we may write the total Hamiltonian [Eq. (2.1)] as

$$H(z_e,z_h,r)=\mathcal{H}_{ij}+\Delta_i^e+\Delta_j^h\ , \tag{2.7}$$

where

$$\Delta_i^\sigma=V_1^\sigma(z_\sigma-s_1)+V_2^\sigma(z_\sigma-s_2)-V_i^\sigma(z_\sigma-s_i)-q_\sigma FC_i^\sigma(z_\sigma)\ , \tag{2.8}$$

and

$$C_i^\sigma(z)=\begin{cases}z+L_i/2 & \text{if } z<s_i-L_i/2\\ s_i & \text{if } |z-s_i|\le L_i/2\\ z-L_i/2 & \text{if } z>s_i+L_i/2.\end{cases} \tag{2.9}$$

The term Δ_i^e (Δ_j^h) describes the CDQW band offset potential with the ith (jth) well for the electron (hole) removed. It also includes the effect of the electric field outside the ith (jth) well (see Fig. 2). These Δ^σ terms lead to a coupling between the eigenstates of the $\mathcal{H}_{ij}$.

We denote the electric-field-dependent ground states of the two-well Hamiltonians by $\phi_{ij}(z_e,z_h,r)$, where from the form of $\mathcal{H}_{ij}$ we see that the electron (hole) in the state $\phi_{ij}(z_e,z_h,r)$ is localized in the ith (jth) well. We approximate the eigenstates of the *full* Hamiltonian as a linear combination of these four states,

$$\psi_n(z_e,z_h,r)=\sum_{i=1}^{2}\sum_{j=1}^{2}b_{ij}^n\phi_{ij}(z_e,z_h,r)\ , \tag{2.10}$$

where n is the quantum number of the state, and the basis expansion coefficients b_{ij}^n are variational parameters. The condition that the expectation value of the energy be stationary leads to the prescription that H should be diagonalized in the nonorthogonal basis $\phi_{ij}(z_e,z_h,r)$. That is,

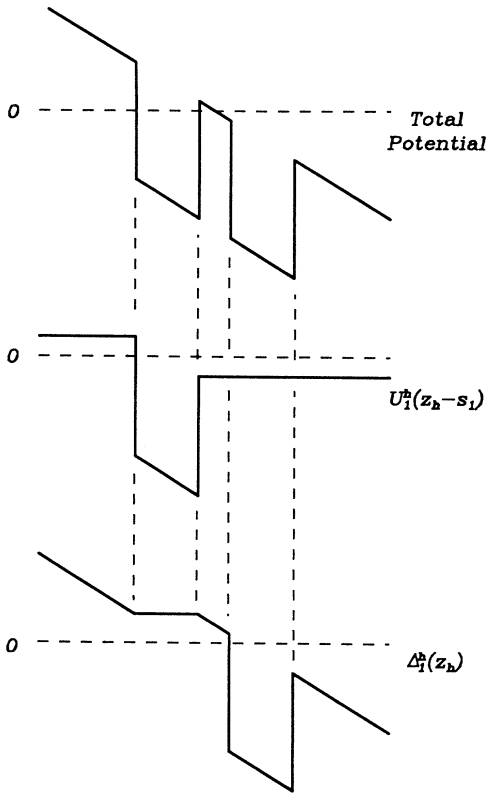

FIG. 2. The splitting of the total hole potential into the sum of the electric-field-dependent well, $U_1^h(z_h-s_1)$, found in the two-well Hamiltonians $\mathcal{H}_{i1}$ and the coupling term Δ_1^h. A similar splitting of the electron portion of the potential is used.

we determine the b_{ij}^n by solving the generalized eigenvalue equation

$$\langle \phi_{lm}|H|\phi_{ij}\rangle b_{ij}^n = E_n \langle \phi_{lm}|\phi_{ij}\rangle b_{ij}^n \ , \tag{2.11}$$

where E_n is the energy of the nth state and, in a manner similar to that of single-particle tight-binding calculations,[27] the Hamiltonian matrix elements may be written as

$$\langle \phi_{lm}|H|\phi_{ij}\rangle = \varepsilon_{ij}\langle \phi_{lm}|\phi_{ij}\rangle + \langle \phi_{lm}|\Delta_i^e + \Delta_j^h|\phi_{ij}\rangle \ , \tag{2.12}$$

where ε_{ij} is the ground-state exciton energy of $\mathcal{H}_{ij}$. The state of lowest energy that we find is obviously our best estimate of the ground state in this basis. Since the higher-energy states are othorgonal to the lowest-energy state and to each other, they are thus the variationally determined excited states.

To implement this procedure we require the ground states of the $\mathcal{H}_{ij}$. Since even they cannot be found analytically, we approximate them by variational solutions of the form

$$\phi_{ij}(z_e,z_h,r) = \left[\frac{2}{\pi}\right]^{1/2} \lambda e^{-\lambda r} f_{ij}^e(z_e - s_i) f_{ij}^h(z_h - s_j) \ , \tag{2.13}$$

where λ is a variational parameter (dependent on i and j) and

$$f_{ij}^{\sigma}(z) = \begin{cases} Ae^{\rho z} & \text{if } z < -L_{\sigma}/2 \\ Be^{-\gamma z}\cos(kz) & \text{if } |z| \le L_{\sigma}/2 \\ Ce^{-\tau z} & \text{if } z > L_{\sigma}/2, \end{cases} \tag{2.14}$$

where γ is the variational parameter (dependent on i and j) that allows the single-particle-like states to adjust due to the presence of the applied electric field and the Coulomb attraction of the particle to its partner. The coefficients A, B, and C are determined by requiring that $f_{ij}^{\sigma}(r,z_e,z_h)$ is normalized and is continuous at layer interfaces. In order to reduce the number of parameters that need to be variationally determined, we set the value of the parameter k to be that found for the lowest eigenstate of a single particle in a finite well in the absence of an electric field. The remaining two parameters ρ and τ are determined via the continuity of $[1/m_{\sigma z}^*(z)](\partial/\partial z)f_{ij}^{\sigma}(z)$ at the interfaces between the given well layer and the adjacent barrier layers. Since $f_{ij}^{\sigma}(z)$ is small at the remaining interfaces, we make the approximation that its derivative is continuous there; this simplifies the calculation substantially. When there is no applied electric field, we find that the improvement in the energy by having nonzero γ's is very small unless the wells are wide ($\gtrsim 100$ Å), very narrow ($\lesssim 10$ Å), or very shallow.[15] We note that because we are not finding the exact ground states of the $\mathcal{H}_{ij}$ Eq. (2.12) is no longer exact unless $(ij)=(lm)$. However, we proceed by continuing to use Eq. (2.12) with

$$\varepsilon_{ij} \equiv \langle \phi_{ij}|\mathcal{H}_{ij}|\phi_{ij}\rangle \ , \tag{2.15}$$

thereby removing the problem of calculating the difficult Coulomb integrals between different states. We have previously discussed the validity of this approximation.[15] Before proceeding, we note that in the presence of a nonzero F there is, strictly speaking, no ground state for H, and the states form a continuum. Thus, for the single-particle states many authors have addressed this problem in the CDQW by using a resonant tunneling method.[28] Now for single-particle states in *single* quantum wells, the variational wave functions [Eq. (2.14)] yield essentially identical results to the resonant tunneling method for the field strengths considered here.[29] The inclusion of excitonic effects in the resonant tunneling method would be prohibitively complicated, as there would be a strong Coulombic mixing between the single-particle states. We therefore proceed with Eq. (2.13) as our basis, where the Coulombic coupling can be accurately taken into account.

Finally, the oscillator strength per unit area for the state ψ_n is given by[15]

$$f_n = \frac{|F_n(0)|^2|\xi\cdot\mathbf{p}_{cv}|^2}{m_0 E_n} \ , \tag{2.16}$$

where $\mathbf{p}_{cv}$ is the momentum matrix element between the bulk conduction- and valence-band Bloch states at the band extrema, m_0 is the free-electron mass, ξ is the electric field polarization vector, and the electron-hole overlap $F_n(0)$ is given by

$$F_n(0) = \int dw\ \psi_n(z_e = w, z_h = w, r = 0) \ . \tag{2.17}$$

III. SYMMETRIC COUPLED WELLS WITH $F=0$

The problem of determining the exciton states in a symmetric CDQW has recently been tackled by a number of authors,[10,12–14] several of whom have considered the effects of an applied electric field.[10,12,14] To illustrate the advantages and disadvantages of our method, we first discuss the results in the absence of an applied electric field.

In Fig. 3 we present our results for the energies of all four lowest 1s exciton states relative to the band gap of the well material as a function of barrier width, L_b, for a well width of $0.6a_0$, where $a_0 = \hbar^2\epsilon/(\mu e^2)$ is the exciton

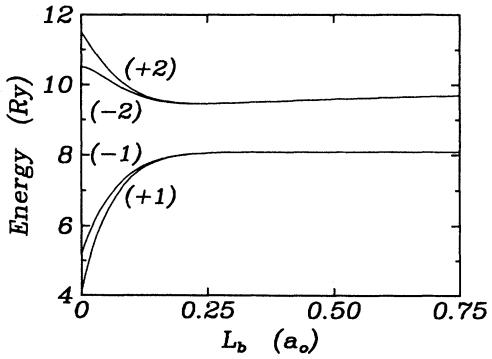

FIG. 3. The energies of the four lowest 1s exciton states, relative to the well band gap energy, as a function of barrier width for the structure of KM with $L_1 = L_2 = 0.6a_0$. The quantum number n of the states is in parentheses beside each curve.

Bohr radius and $\mathrm{Ry}=\hbar^2/2\mu a_0^2$ is the exciton Rydberg in the well material. For comparison purposes, we use the parameters of Kamizato and Matsuura[12] (hereafter referred to as KM), which correspond roughly to those of a $GaAs/Ga_{0.7}Al_{0.3}As$ structure. It will be convenient in the following discussion to divide the range of barrier widths into three regimes: narrow, with $L_b \lesssim 0.13a_0$; intermediate, with $0.13a_0 \lesssim L_b \lesssim 0.5a_0$; and wide, with $L_b \gtrsim 0.5a_0$.

In the approximation that the Coulomb attraction between the electron and the hole is neglected (noninteracting-particle picture), one can separately label the electron and hole states as either symmetric (+) or antisymmetric (−) under inversion. The noninteracting electron-hole pair states are then products of hole (h_+ or h_-) and electron (e_+ or e_-) single-particle states. These noninteracting pair states are nondegenerate for all barrier thicknesses. We find that this is also the case when the Coulomb attraction is taken into account (exciton states). Thus, due to the inversion symmetry of Hamiltonian, the *exciton* states must be either symmetric or antisymmetric under the operation $(z_e,z_h)\rightarrow(-z_e,-z_h)$. This tells us that for the symmetric states (positive parity), $b_{11}=b_{22}$ and $b_{12}=b_{21}$, while for the antisymmetric states (negative parity), $b_{11}=-b_{22}$ and $b_{12}=-b_{21}$. As is expected from examining the symmetry of the pair states in the noninteracting limit, the first and fourth exciton states in order of increasing energy are symmetric, while the second and third are antisymmetric. To simplify notation we will denote the states (in this order) by $n=\{+1,-1,-2,+2\}$, where the sign before each index denotes the parity of the state. For narrow barriers, these roughly correspond, respectively, to the noninteracting pair states: $\{(h_+e_+),(h_-e_+),(h_+e_-),(h_-e_-)\}$, although, as we shall show, no such precise assignment is possible due to the strong Coulombic coupling between the single-particle states. In the absence of an applied electric field, the only accessible states are those with overall positive parity, $n=+1,+2$.

For wide barriers, the energy difference between symmetric states and their antisymmetric partners becomes negligible, and so we find $E_{+1}\simeq E_{-1}$ and $E_{+2}\simeq E_{-2}$. However, there is a sizeable difference between E_{+1} and E_{+2} in these structures, a difference that would not be found in the results of calculations that neglect the subband coupling induced by the interaction.[12,14] The source of the difference is easily ascertained by plotting the ratios of the form b_{ij}^n/b_{lm}^n for the four states (see Fig. 4). Consider first the state $n=\pm1$. We see that the ratio $|b_{12}/b_{11}|$ is essentially zero for $L_b \gtrsim 0.5a_0$, indicating [see Eq. (2.10)] a very high probability that the electron and hole are in the *same* layer (intrawell state). Conversely, for the states $n=\pm2$ it is instead the ratio $|b_{11}/b_{12}|$ that is essentially zero in this range of barrier thicknesses, indicating the very high probability that the electron and hole are in different layers (interwell state). This difference in the nature of the two states will lead to very different binding energies, as is evidenced in the separation in energy of the $|n|=2$ levels from the $|n|=1$ levels. Because the binding energy of the interwell states

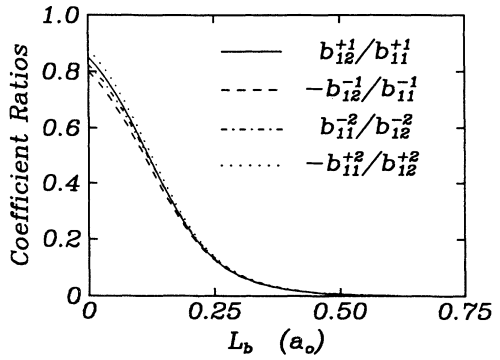

FIG. 4. The two-well ground-state coefficient ratios for the four exciton states as a function of barrier width for the structure of KM with $L_1=L_2=0.6a_0$.

tends to zero as $L_b\rightarrow\infty$, this separation increases with L_b to reach a maximum value equal to the ground-state binding energy. The difference in the nature of the states also shows up in the oscillator strengths, which are plotted in Fig. 5. At large barrier widths the oscillator strength is much greater for the $n=+1$ state than the $n=+2$ state, reflecting the fact that in the former the electron and hole are much more likely to be found at the same position than in the latter.

This large difference is in contrast to the roughly equal oscillator strengths one would obtain from a calculation that neglected subband coupling. Thus, the Coulomb interaction is crucial in establishing the nature of the exciton states in the limit of large barrier widths, L_b, because it causes the electron and hole motion to correlate such that in the ground excition state they are always in the same well. Therefore, in the limit $L_b\rightarrow\infty$, the independent particle picture and nomenclature for the transitions are qualitatively physically unrealistic. In our example of a well width of $0.6a_0$, this occurs for $L_b \gtrsim 0.5a_0$. Quantitatively, from Figs. 4 and 5 we see that the predictions of that picture can be expected to be in significant error for even smaller L_b. Thus, we find that the qualitative behavior of excitons in a CDQW *cannot* be described without subband coupling (cf. the conclusion of KM); the

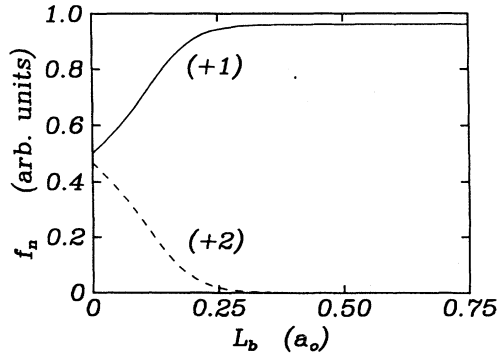

FIG. 5. The oscillator strengths per unit area as a function of barrier width for the two symmetric exciton states for the structure of KM with $L_1=L_2=0.6a_0$. The quantum number n of the states is in parentheses beside each curve.

coupling can change the very nature of the states.

The situation for structures with intermediate barrier widths is somewhat more subtle and complicated as the states are no longer strongly intrawell or interwell in character. In order to illustrate the nature of the ground state in this regime, in Fig. 6 we present our results for the ground-state binding energy as a function of barrier width, for the structure described above, with a fixed well width of $0.6a_0$. The binding energies are given by $E_B = E_{\text{free}} - E_n$, where E_{free} is the noninteracting ground-state energy calculated using the standard transfer-matrix approach.[30] To see the effects of subband coupling, we compare our results with those found using a single-subband variational wave function. We choose for comparison the wave function employed in the first part of KM,

$$\Psi_{ij}^{\text{KM}}(z_e,z_h,r) = e^{-(\lambda r^2+\beta z^2)^{1/2}} \chi_i^e(z_e)\chi_j^h(z_h) , \tag{3.1}$$

where $\chi_1^\sigma(z)$ [$\chi_2^\sigma(z)$] is the symmetric ground state (antisymmetric excited state) of the σ particle in the double-well structure, and λ and β are variational parameters. The results for the binding energy using this wave function are presented in Fig. 6 (dashed line). Comparison shows that our method yields larger binding energies for the ground state than that of Eq. (3.1) for the range of barrier thicknesses, $0.1a_0 < L_b < 1.8a_0$. As can be seen, for some values of L_b in the intermediate barrier regime, our binding energies are greater by as much as 0.45 Ry ($\simeq 2$ meV for GaAs).

In the same figure, we also present as a dotted line the results obtained by coupling the Ψ_{ij}^{KM} from different subbands (ij) of Eq. (3.1) as calculated by Kamizato and Matsuura near the end of KM. We shall refer to this as the KM subband-coupling method. As can be seen, the results of this calculation are in good agreement with ours for $L_b \gtrsim 0.1a_0$. We have seen already that the qualitative nature of the states in the wide barrier regime can be changed drastically when coupling between the different subbands is accounted for. Since the KM subband-coupling method and our method yield similar results, we compare *our* wave function [Eq. (2.14)] with the wave function of Eq. (3.1) to study the importance

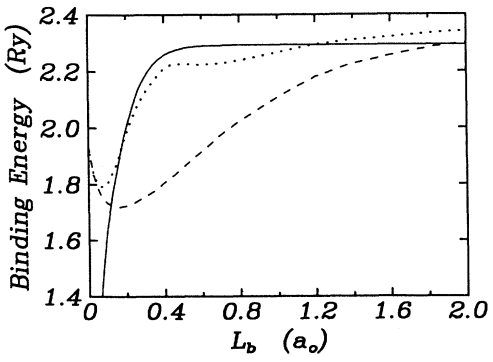

FIG. 6. Binding energy as a function of barrier thickness for the structure of KM with $L_1 = L_2 = 0.6a_0$. The solid line is our result. The other two lines are the results of KM with (dotted) and without (dashed) coupling to their excited states.

and nature of the subband coupling in the intermediate barrier regime.

Solely for the sake of simplifying the discussion, we make a tight-binding approximation for the single-particle wave functions and write

$$\chi_1^\sigma(z) \simeq f_1^\sigma(z_\sigma - s_1) + f_2^\sigma(z_\sigma - s_2) . \tag{3.2}$$

Then the ground-state wave function of Eq. (3.1) is written as

$$\Psi_{11}(z_e,z_h,r) \simeq e^{(-\lambda r^2+\beta z^2)^{1/2}}[(f_1^e f_1^h + f_2^e f_2^h) + (f_1^e f_2^h + f_2^e f_1^h)] , \tag{3.3}$$

where f_i^σ is the single-particle eigenstate for a particle in the ith well [Eq. (2.14) with $\gamma = 0$]. Using the same notation and setting the variational parameters γ to zero, *our* wave function can be written:

$$\psi_{\pm n}(z_e,z_h,r) = b_{11}^{\pm n}(f_1^e f_1^h \pm f_2^e f_2^h)e^{-\lambda_s r} + b_{12}^{\pm n}(f_1^e f_2^h \pm f_2^e f_1^h)e^{-\lambda_d r} , \tag{3.4}$$

where $\lambda_s \neq \lambda_d$ and $n > 0$. Now consider Eqs. (3.3) and (3.4), and neglect for the moment the effect of the exponential factors; also ignore for now the differences between the electron and hole effective masses and potentials, so that f_i^e and f_i^h can be thought of as identical. Note that the wave function (3.3) is analogous to the two-particle wave function that one would write down for a diatomic molecule in a simple molecular-orbital picture.[31] The functions f_1 and f_2 play the role of atomic orbitals, and χ_1 that of the ground-state molecular orbital constructed from them [Eq. (3.2)]; both particles are then put in the same molecular orbital [see Eq. (3.1)] to form the ground-state wave function. This then contains equal amplitudes of configurations in which the two particles are at the same site $(f_1^e f_1^h, f_2^e f_2^h)$, and configurations in which they are at different sites $(f_1^e f_2^h, f_2^e f_1^h)$. In a two-electron problem such as a diatomic molecule, these would be referred to as "ionic" and "covalent" configurations, respectively. Here, since we have particles of opposite charge—an electron and a hole—in a corresponding notation, the configurations would be referred to as "nonpolar" and "polar." The more usual notation for these, of course, describes them, respectively, as "intrawell" and "interwell" configurations.

Now, in the other simple model for a diatomic molecule, due to Heitler and London,[31] only the covalent configuration is kept; in may cases this leads to a better estimate of the ground-state energy than including the ionic configuration with equal amplitude, as is done in the simple molecular-orbital picture. Certainly, in the limit that the atoms are separated by a large distance, the contributions to the true wave function from the ionic configurations in negligible. In general, though, it is better to variationally determine the amplitudes of the ionic and covalent configurations, rather than arbitrarily setting them equal (molecular orbital), or neglecting one completely (Heitler and London[31]).

In our case of an electron and hole, which attract rather than repel, it is the nonpolar, intrawell configuration

that increasingly dominates the ground state for larger well separation (barrier thickness), as discussed above. But for intermediate barrier thicknesses it is clear, by analogy with the diatomic molecule problem, that it is better to variationally determine the amplitudes of the interwell and intrawell configurations [Eq. (3.4)] than to arbitrarily set them identical [Eq. (3.3)]. This largely explains why we obtain larger binding energies (solid line, Fig. 6) than those found using (3.1) (dashed line) at all but the smallest barrier thicknesses ($L_b \lesssim 0.17a_0$). Nonetheless, the analogy with simple models for the physics of diatomic molecules is not complete because of the exponential factors in Eqs. (3.3) and (3.4). In particular, for very wide barriers, the results found using Eq. (3.1) improve greatly because the exponential factor associated with the electron-hole separation in the z direction [the β term in the exponential in Eq. (3.3)] effectively removes the interwell configurations. At these large separations, the wave function (3.1) used by KM becomes similar to ours.

We now turn to consider the nature of the radial dependence of the states in the intermediate barrier regime. In a paper by Galbraith and Duggan[13] (hereafter referred to as GD), the problem of finding the ground-state energy in the intermediate barrier regime was tackled by employing a variational wave function of the form

$$\psi^{\mathrm{GD}}(z_e,z_h,r)=e^{-\lambda r}\sum_{i=1}^{2} a_i\chi_i^e(z_e)\sum_{j=1}^{2} c_j\chi_j^h(z_h)\ , \tag{3.5}$$

where λ and the a_i and c_i are variational parameters. This is considerably simpler than the wave function we employ [Eq. (2.10), or (3.4) if the γ's are set to zero], particularly because only one exponential factor is involved. Although the wave function (3.5) does allow for the coupling between single-particle states, it suffers from two serious flaws. The first is that it yields states of incorrect symmetry (see the discussion on symmetry at the beginning of this section) for large values of L_b. More importantly, it treats the radial behavior in a way that does not account for the three-dimensional nature of the state.

This can be understood by imagining the χ_i^σ of Eq. (3.5) expanded in a single-well basis as in Eq. (3.2). Then both intrawell and interwell terms will appear in Eq. (3.5) with the same exponential factor. But because the Coulomb interaction is much larger when evaluated over an intrawell term than over an interwell term, we except a much faster radial decay in the former than in the latter. Indeed, this behavior is given by our wave functions, as demonstrated in Fig. 7, where we show $\langle r \rangle$ as a function of L_b. For the states of large interwell character ($n=\pm 2$ for large L_b), $\langle r \rangle$ is much larger than those of large intrawell character ($n=\pm 1$ for large L_b). The source of this difference is the difference between λ_s and λ_d. Since this variational degree of freedom is not present in the wave function of GD, that approach, which has also been commonly used in superlattice calculations,[16,17] is only reasonable when the wave function is either primarily of pure interwell or intrawell type. This will not be the case in small barrier structures or when an electric field is applied, as we shall show in the next section.

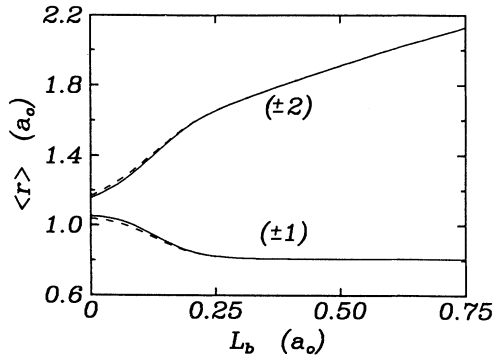

FIG. 7. The expectation value of the in-plane electron-hole separation, $\langle r \rangle$, as a function of L_b for the four states for the structure of KM with $L_1=L_2=0.6a_0$. The quantum number n of the states is in parentheses beside each curve with the solid lines corresponding to the symmetric states and the dashed lines to the antisymmetric ones.

We now consider the narrow barrier regime $L_b \lesssim 0.13a_0$. For these thicknesses, our binding energy becomes much smaller than that of the KM subband-coupling method (Fig. 6). This can be traced to the breakdown of the tight-binding approximation used in our calculation, by comparing the results of single-particle tight-binding calculations with those of more exact treatments. For this structure with $L_b=0.13a_0$, the energy calculated via the tight-binding (TB) method is lower than the exact result for a noninteracting electron-hole pair by $\Delta E_{\mathrm{TB}} \simeq 0.06$ Ry. This deficiency is due to the fact that the tight-binding method cannot completely capture the tendency of the electron to lower its kinetic energy by delocalizing. This, then, sets a lower limit on the barrier thicknesses that can be treated by our approach. No such problem is encountered in the methods that use the noninteracting electron-hole pair states as the basis.[12,13] However, one need not perform such a calculation to see what the lower limit on L_b is for our method; this limit can easily be ascertained by examining *single-particle* behavior alone.

We now present a brief comparison of the our method with the KM subband-coupling method. We note that because of the approximation we have made in calculating our matrix elements [Eq. (2.15)], our calculation is not strictly variational. However, it appears that our method gives a slightly more accurate ground-state binding energy for $0.17a_0 \leq L_b \leq 1.2a_0$ than the configuration mixing method of KM. In the small barrier regime ($L_b \gtrsim 0.13a_0$), the method of KM is clearly superior as our method breaks down. This will also be the case in any CDQW where a tight-binding method is insufficient. When tight binding is sufficient, however, we feel that our method is both *physically* and *computationally* the simpler approach, for all the states. Physically, we see from Fig. 4 that down to about $L_b \simeq 0.25a_0$, the exciton eigenstates are still *primarily* interwell or intrawell in nature. Since our basis states are either interwell or intrawell states [see Eqs. (2.13) and (2.14)], it is physically more clear to begin with them rather than with the Ψ_{ij} of

KM, which in the range of intermediate barrier thicknesses are neither primarily interwell nor intrawell. Computationally, our method is the much simpler approach. Except in the cases where $L_i \gg a_0$, without serious error the variational γ's in our wave function can be set to zero, leaving only one variational parameter to be calculated for each basis state; there are two essential variational parameters for each of the basis states of KM. Even neglecting this fact, the evaluation of the Hamiltonian matrix elements for the wave functions of KM are much more involved than ours because our basis states are of a far simpler functional form and we can use the simplification of the tight-binding approximation [Eqs. (2.12) and (2.15)].

Finally, we close this section by mentioning that a variational wave function that should be better than any of the above when there is no applied electric field and the wells are not too shallow or wide [such that the γ's in Eq. (2.13) can be set to zero] is

$$\Psi(z_e,z_h,r)=[A(\chi_1^e\chi_1^h+\chi_2^e\chi_2^h)+B(\chi_1^e\chi_2^h+\chi_2^e\chi_1^h)]e^{-\lambda_s r} +[C(\chi_1^e\chi_1^h-\chi_2^e\chi_2^h)+D(\chi_1^e\chi_2^h-\chi_2^e\chi_1^h)]e^{-\lambda_d r}, \tag{3.6}$$

where we have omitted the explicit dependence of χ_i^σ on z_σ for simplicity. It is easy to show from symmetry arguments that $B=D\equiv 0$ for the symmetric states, and $A=C\equiv 0$ for the antisymmetric states, unless a static electric field is applied. This wave function allows the simultaneous calculation of the four lowest $1s$ exciton states, takes the kinetic energy into account properly, and treats the states in the proper quasi-three-dimensional manner for all barrier thicknesses. It is computationally much more involved than our method, but still considerably simpler than the subband-couplng method of KM. Generalization of this wave function to the case of a superlattice leads to the concept of the exciton Wannier function, which we have discussed in previous papers.[15,20] What we have done here and in those papers is develop an approximation to these functions that simplifies the calculation enormously. Without these simplifications the method becomes even more complicated when we apply a static electric field, as the wave function of Eq. (3.6) then requires the inclusion of all four terms with a separate exponential factor for each. We feel that this method would only then be worth the effort for very narrow barrier structures. We finally point out that of all the methods mentioned above, only our method can be reasonably generalized for application in superlattices,[15,20,21] as the basis and number of variational parameters needed for the other methods would be far too large to be practical.

IV. ELECTRIC FIELD DEPENDENCE

In the preceding section we defined narrow, intermediate, and wide barrier regimes for the particular CDQW parameters we were considering. Based on the physics that was revealed in analyzing our results and comparing them to the results of others, we now redefine those regimes more generally, in agreement with our earlier definitions but in a way that will apply to any CDQW.

By the *narrow barrier regime* we refer to barriers so narrow that a tight-binding approach cannot satisfactorily describe the single-particle states in the CDQW. In this regime, our method is inadequate. For slightly thicker barriers, we expect in general the exciton states to all have (in the absence of a static electric field) nonnegligible intrawell *and* interwell character. This we refer to as the *intermediate barrier regime.* Finally, for wide enough barriers, the exciton states are essentially exclusively interwell or intrawell in character. This we refer to as the *wide barrier regime.* The boundary between the intermediate and wide barrier regimes can be determined by examining the energy separation between the single-particle symmetric and antisymmetric states; when the barrier width is wide enough such that these energy differences become small relative to the Coulomb interaction energy, strong intermixing of single-particle states will occur, indicating that one has moved from the intermediate to the wide barrier regime.

Our method is applicable throughout the wide and intermediate barrier regimes, although for extremely wide wells ($L_b \gg a_0$) it would be necessary to choose more general basis functions than the ϕ_{ij} of Eq. (2.13). The crucial point is that the approach does not become inaccurate, as does that of GD, if the states have significant interwell *and* intrawell character; nor does it become excessively complicated, as does that of KM, if the states have exclusively interwell *or* intrawell character. Thus it is an ideal approach for calculating the exciton states in a CDQW in the presence of a static electric field, where the whole range of excitonic character can be accessed. We begin the examination of these systems in this section by presenting some results for the electric field dependence of the lowest four $1s$ exciton levels for three different symmetric CDQW structures. Despite the extreme changes in the nature of the states as the electric field strength is increased, for lack of a better labeling system we label the states by their $F=0$ quantum numbers, n (see the discussion at the start of Sec. III) recognizing the fact that for $F\neq 0$ the states are far from being eigenstates of parity.

For comparison, we first present the results for the structure of GD, i.e., $L_1=L_2=L_b=50$ Å, a structure that is comfortably in the wide barrier regime. For our calculation, we use all of the physical parameters given in GD, and for the overall band offset (not given in GD) we use $v_e+v_h=488$ meV, a value that is in the middle of the generally accepted range for that value of x (see, e.g., Refs. 22, 23, 25, and 32). In Fig. 8 we present the energy levels along with the results of GD for the state that evolves from the $F=0$ ground state. It is clear that the blue shift predicted in GD is not found using our method. By examining in some detail the difference in the behavior of the two wave functions, the source of this discrepancy can be understood. From the plots of $\langle z_e \rangle_n$ and $\langle z_h \rangle_n$ as a function of F (Fig. 9), we find that over the range of F for which the energy of GD is blue shifted, our ground-state wave function has an interwell expansion coefficient that is a sizable fraction of the large intrawell

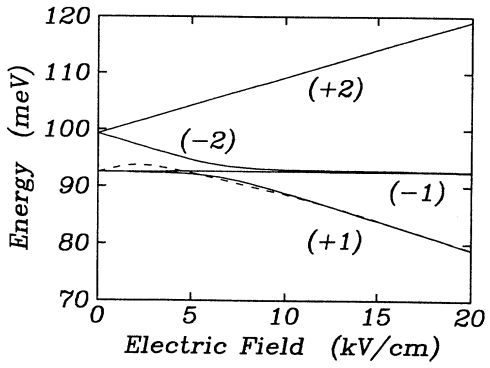

FIG. 8. Exciton energies as a function of electric field for the four exciton states of the Ga-Al-As system of GD for which $L_1=L_2=L_b=50$ Å. The solid lines are our results and the dashed line is the result of GD for the lowest state, which shows a blue shift according to their calculations. The energy curve for the result of GD has been set so that $F=0$ energy matches ours since no value for this quantity was given in GD. The quantum number n of the states is in parentheses beside each curve.

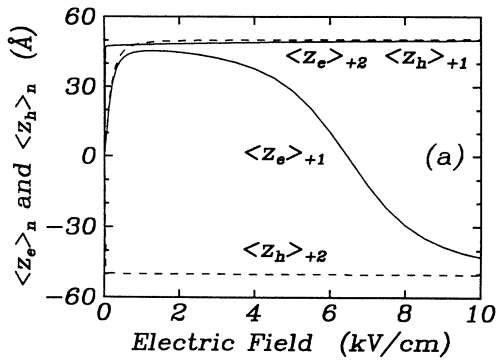

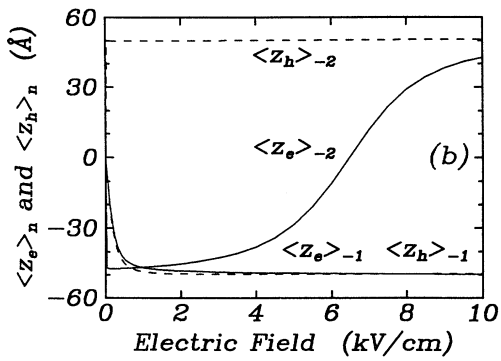

FIG. 9. The expectation values $\langle z_e \rangle_n$ (solid lines) and $\langle z_h \rangle_n$ (dashed lines), of the electron and hole coordinates along the growth direction as a function of electric field for (a) the $n=+1,+2$ exciton states and (b) the $n=-1,-2$ exciton states of the Ga-Al-As system of GD for which $L_1=L_2=L_b=50$ Å. The particular expectation value is given parentheses beside each curve. Note that all of the expectation values go to zero when $F\rightarrow 0$.

coefficient ($|b_{12}^{+1}/b_{22}^{+1}|\simeq 0.22$ for $F=2.0$ kV/cm). Examining the expectation value of r as a function of F (Fig. 10), we see that the radial separation for the interwell states is approximately *twice* that of the intrawell states. Thus the wave function of GD, which *forces* the radial behavior of the two portions of the wave function to be the same, is not able to account for the three-dimensional nature of the state in the manner of our wave function. As a result, it underestimates seriously the binding energy. It should be pointed out that, since there is strictly speaking no ground state once an electric field is applied, finding a lower energy for the $n=+1$ state does not necessarily indicate a better estimation of the energy. Thus one should be careful in trying to draw too much from the comparison, particularly when the field is large. However, even the examination of the repulsion of the exciton energy levels (Fig. 8) leads one to the conclusion that there should be no blue shift in the $n=+1$ level.

This demonstrates how careful one must be when trying to draw general conclusions from the results of a variational calculation in these multiwell structures. It is essential that the wave functions are flexible enough to allow for subtle changes in the radial behavior as a given system parameter is changed. It appears that the single exponential product states commonly used in CDQW's [Eq. (3.5)] and superlattices are not sufficiently complicated to capture these features.

We now examine the nature of all of the exciton states as a function of field strength. From Fig. 9 we see that for $F=0$ all of the states have zero dipole moment. Once a field is applied, the symmetric states mix almost immediately with their nearly degenerate antisymmetric partners, yielding two states of primarily interwell character ($n=\pm 2$) and two of primarily intrawell character ($n=\pm 1$). When the field strength becomes larger, there is a strong interaction between the $n=-2$ and the $n=+1$ states in the field range $1\rightarrow 10$ kV/cm. The electrons in these two states change places; the result is that the two states exchange character in a way that is similar to that which occurs in the exciton Stark ladder,[20,21] although here there are only four states instead of an

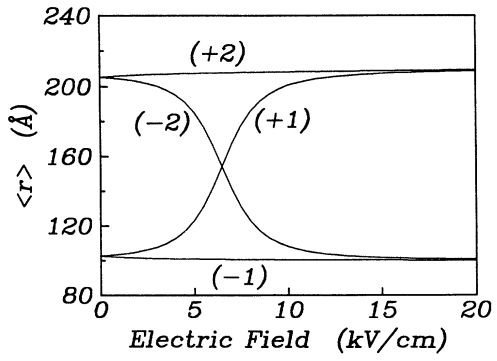

FIG. 10. The expectation value of the in-plane electron-hole separation, $\langle r \rangle$, as a function of electric field for the four states of the Ga-Al-As system of GD for which $L_1=L_2=L_b=50$ Å. The quantum number n of the states is in parentheses beside each curve.

infinite number. In order to show the very different radial behavior of intrawell- and interwell-type states and how this behavior changes with field, in Fig. 10 we plot $\langle r \rangle$ as a function of F. As can be seen, the expectation value of the radial separation of the electron and hole is much larger in the interwell states ($n=-2$ for $F \lesssim 5$ kV/cm, $n=+1$ for $F \gtrsim 10$ kV/cm, and $n=+2$ for all fields) than it is in the intrawell states ($n=+1$ for $F \lesssim 5$ kV/cm, $n=-2$ for $F \gtrsim 10$ kV/cm, and $n=-1$ for all fields).

In Fig. 11 we present the oscillator strengths of the various states as a function of field for this same structure. As is expected, the ground state ($n=+1$) and the highest excited state ($n=+2$) very quickly lose most of their oscillator strength as they transform into interwell states. The two intermediate states, on the other hand, pick up oscillator strength as they transform into intrawell states, with the electron and hole both localized in either the right (ψ_{-2}) or left (ψ_{-1}) wells. We note that, because of the expected low level of coupling between these four states and the rest of the exciton states for moderate electric fields, it can easily be shown that the sum of the oscillator strengths for the four states should be approximately independent of field strength. This is precisely what we find. If, however, the field is strong enough such that the quantum confined Stark effect for a single well in appreciable, then the sum of the oscillator strengths will slowly decrease with increasing field. Finally, it is clear from the figure that it is not enough to simply track the energy level of the ground state, for this is an essentially nonabsorbing state for field strengths greater than 10 kV/cm, while the other states are strongly absorbing.

We now examine the results for a structure that is in the intermediate barrier regime: the $GaAs/Ga_{0.7}Al_{0.3}As$ system of Chen *et al.*,[5] which has nominal barrier and well widths of $L_b=18$ Å and $L_1=L_2=75$ Å. In Fig. 12 we present our calculated results for the energy levels of the four heavy- and four light-hole 1*s*-exciton states, along with the experimentally measured photocurrent-peak spectra of Chen *et al.*[5] In our calculation we use the band offsets $v_e=240$ meV, $v_h=120$ meV, the effective masses in GaAs, ($Ga_{0.7}Al_{0.3}As$) of $m_e^*=0.0665$ (0.085), $m^*_{\mathrm{hhz}}=0.34$ (0.43), $m^*_{\mathrm{hh}\|}=0.115$ (0.165), $m^*_{\mathrm{lhz}}=0.094$ (0.136), $m^*_{\mathrm{lh}\|}=0.206$ (0.279), a static dielectric constant of $\epsilon=12.5$, and the generally accepted value of 1.519 eV for the band gap of GaAs at 4 K. The transverse effective masses are obtained by using their relation to the longitudinal effective masses via the Luttinger parameters.[33] We use layer thicknesses of $L_1=L_2=64$ Å and $L_b=14$ Å, which are in very close agreement with the new experimental estimates of $L_1=L_2=64$ Å and $L_b=15$ Å.[14] Finally, using the information given in Chen's paper, we have mapped the applied voltage onto the electric field using the relation $F=-52.03\ \mathrm{V}+81.43$. We note that all of the parameters used are in good agreement with the generally accepted values except for the value of 0.136 for m^*_{lhz}, which is somewhat higher than generally expected. We point out, however, that we found it necessary to use this same value when modeling a superlattice Stark ladder.[21]

As can be seen, the agreement is generally very good, especially considering that this structure is very close to being in the small barrier regime ($\Delta E_{\mathrm{TB}} \simeq 1$ meV). Even the curvature of the -1 and -2 energy lines at high field, due to the essentially single-well quantum confined stark effect, is reasonably well accounted for. The only serious deviation of theory from experiment is for the $n=-1$ light-hole state at low electric fields—a deviation that has appeared in other calculations[14] and that we cannot explain at present.

The behavior of the states as a function of field is similar to that of the $L_1=L_2=L_b=50$ Å structure discussed above. The only essential difference arises from the fact that the states at $F=0$ are of mixed intrawell and interwell character (see Fig. 4). As one expects from the larger $F=0$ splitting of the $\pm n$ states, the mixing of these states continues to higher fields than in the wide barrier structure. This is evidenced by the almost quadratic curving of the $n=+2$ states in this structure as contrast-

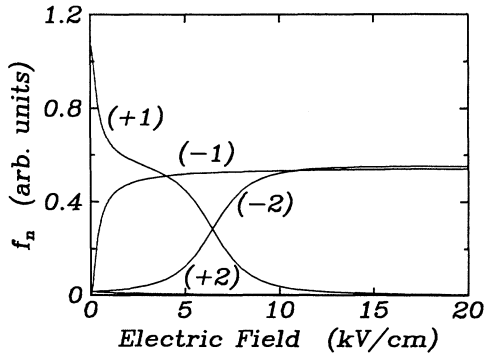

FIG. 11. Oscillator strength f_n per unit area as a function of electric field for the four states of the Ga-Al-As structure of GD for which $L_1=L_2=L_b=50$ Å. The quantum number n of the state is given in parentheses beside each curve (the oscillator strength for the $n=+2$ state is nearly zero).

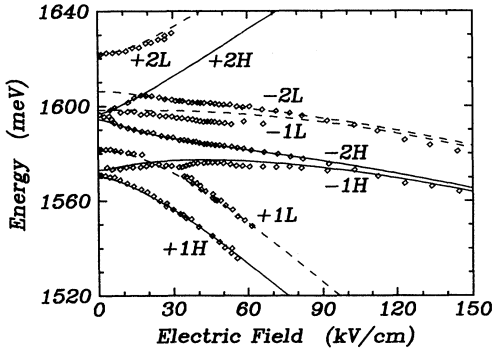

FIG. 12. Calculated energy levels of the heavy-hole (solid lines) and light-hole (dashed lines) exciton states as a function of electric field for the experimental symmetric Ga-Al-As structure of Chen *et al.* (Ref. 5). The lines denote our theory while the diamonds denote the experimental results. The quantum label of each state is given beside the curve, where nH (nL) denotes the nth heavy- (light-) hole exciton state.

ed to the seemingly linear behavior in the wide barrier structure.

A calculation of the excitonic spectrum for the above structure was recently performed by Lee *et al.*[14] Their method, however, utilizes several approximations more extreme than the ones we adopt here. First, they do not allow for mixing between the different single-particle states. For wider barrier structures, this would lead to poor results, even the absence of an electric field. Second, and of more concern with respect to the structure being discussed, their basis states are constructed from the field-dependent eigenstates of a double-well system placed in the center of an infinite potential well. Thus, when an electric field is applied, the derived eigenstates have an appreciable probability of being found outside of the double-well region (Fig. 6 of that paper). Although these may be good approximations to the exact single-particle states, it seems very likely that the electron-hole attraction would mix these single-particle states rather strongly with many of the other eigenstates—particularly the ones that have energies close to these—to remove the long oscillating tails and thereby decrease the electron-hole separation. This apparent problem with the method is seen clearly in Figs. 7(d) and 11(b) of that paper, where the $12H$ state pulls away from the $21H$ state, in disagreement with the data[5] and with what we find.

Finally, in order to demonstrate the effects of the electron-hole interaction on the energy levels and to demonstrate the accuracy of our wave function, we present in Fig. 13 the results of the shooting-method calculation of Bloss[32] for the *noninteracting* electron-hole transition energies for the system with $L_b=18$ Å, $L_1=L_2=70$ Å. In the same figure we also present our exciton results for the same system, using the parameters of Bloss with $\epsilon=12.5$ and the in-plane masses determined using the relationships between the hole masses and the Luttinger parameters.[33] We note that, like the last structure, this CDQW is on the border between the narrow and intermediate barrier regimes, with $\Delta E_{\rm TB}\simeq 0.6$ meV. To aid in the comparison, *we have shifted the results of Bloss up by 7.26 meV* so that the $F=0$ ground-state energies match. This difference in the energies is due to the exciton binding energy, which is found in our calculation but not in that of Bloss. Because all of the eight states at $F=0$ have roughly equal intrawell and interwell character, the binding energies for all the states are approximately equal and so Bloss' values *after the energy shift* for the $F=0$ energies agree rather well with ours. However, even in this system where the barrier is so narrow (and hence the binding energies are relatively low), the deviation of the two sets of curves as a function of F is nonnegligible ($\simeq 3$ meV). At large fields the energies of the light- and heavy-hole $+1$ and $+2$ states are higher in our calculation then in Bloss's because the states have become more interwell in character and hence the binding energy has decreased from its $F=0$ value. For the other states, our energies are generally lower than those of Bloss at fields up to 70 kV/cm because the states have become more intrawell-like at higher electric field strengths and hence their binding energies have decreased relative to those at $F=0$. At still higher fields our states become higher in energy than those of Bloss; this is due to the decrease in binding energy as the quantum confined Stark effect begins to separate the electron and hole in these intrawell states.

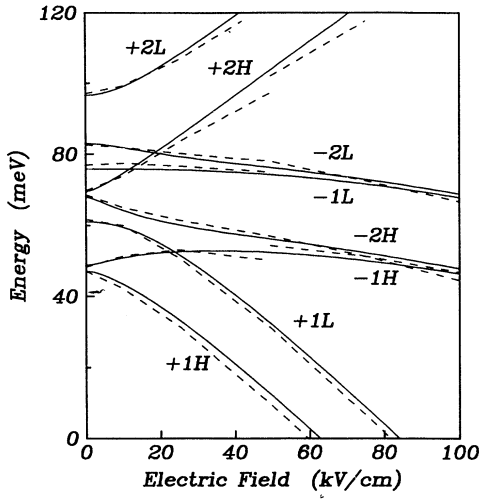

FIG. 13. Energy of the heavy- and light-hole transitions as a function of electric field for the structure of Bloss (Ref. 32) with $L_w=70$ Å and $L_b=18$ Å. The solid lines are our exciton results while the dashed lines are the results of the single-particle calculation of Bloss, where we have *shifted up* the latter set of curves by the $F=0$ heavy-hole exciton ground-state binding energy ($\simeq 7.26$ meV) to allow a more-direct comparison of the subtle effects of the exciton binding. The quantum label of each state is given beside the curve, where nH (nL) denotes the nth heavy- (light-) hole exciton state. The discontinuities in some of the energy lines for the results of Bloss are the result of coupling between the antisymmetric single-particle heavy-hole state with a higher heavy-hole state. This effect is not taken into account in our calculation.

Because for $F=0$ the states are neither interwell nor intrawell states, these deviations in the field behavior of the exciton energy levels from the noninteracting transition energies are only about half the $F=0$ ground-state binding energy. They would be much larger for a system with larger barriers ($L_b\gtrsim 35$ Å) where at $F=0$ the ground state is primarily intrawell while at large F it is primarily interwell. For example, from Fig. 3 it is apparent that the difference between an interwell and an intrawell state binding energy is approximately 1.5 Ry ($\simeq 7$ meV) for a CDQW with $L_b=0.25a_0$ ($\simeq 35$ Å) and $L_w=0.6a_0$ ($\simeq 80$ Å). Hence a calculation that ignores the Coulomb interaction for this system could not reproduce the excitonic results with a simple rigid shift to match the $F=0$ energies; if this were done, some of the high field levels would be off by as much as 7 meV.

V. AN ASYMMETRIC TWO-WELL STRUCTURE

In this section, we present the results for a structure in which there is a sizable separation of the electron and hole (and hence a sizeable permanent dipole moment) for the ground state even in the absence of an applied electric field. The structure is of the form shown in Fig. 1: that

is, $v_\sigma^1 > v_\sigma^2$ and $L_1 < L_2$. The charge separation arises because the hole, being heavy, finds it energetically favorable to reside primarily in the lower potential of the first layer, even though that layer is narrow. The electron, on the other hand, has a confinement energy in the first well that is so large it essentially counteracts the lower potential of that well. As a result, the electron has a reasonably high probability of being found in the second well. The structure that we examine has layer thicknesses of $L_1 = 40$ Å, $L_2 = 55$ Å, $L_b = 35$ Å; band offsets of $v_e^1 = 300$ meV, $v_e^2 = 271$ meV, $v_h^1 = 148$ meV, $v_h^2 = 133$ meV; effective masses in the wells (barriers) of $m_e^* = 0.0665$ (0.084), $m_{hz}^* = 0.34$ (0.476), and $m_{h\|}^* = 0.19$; and a dielectric constant of $\epsilon = 12.4$. This corresponds to a $GaAs/Ga_{1-x}Al_xAs$ system where $x \simeq 0.35$ in the three barrier regions, $x = 0.0$ in the first well layer, and $x \simeq 0.04$ in the second well layer.

The energy of the four exciton states as a function of field strength is given in Fig. 14. For lack of a better labeling system for this complicated system, we label the states in order of increasing energy by $n = 1,2,3,4$. As can be seen, the ground state (solid line) has a permanent dipole moment at $F = 0$. The expectation values $\langle z_e \rangle$ and $\langle z_h \rangle$ of the electron and hole in the ground state are shown in Fig. 15. For $F = 0$, the hole is essentially in the center of the first (left) well while the expectation value of the position of the electron is somewhat right of center. This system is similar to the "asymmetric" well proposed by previous authors[34] for *intersubband* transitions, but we find that for our structure the addition of the barrier enhances the electron-hole separation in the ground state, and hence results in an enhanced Stark shift at low electric field strengths. Thus, although this structure is well out of the narrow barrier regime, even in zero field, the states have both a strong interwell and intrawell character. The oscillation of the electron position of the ground state as a function of electric field is a strictly excitonic effect. For $F = -20$ kV/cm, the electron is primarily in the second well while the hole is primarily in the first. As the field is made less negative, the hole is stationary while the electron moves toward the second well. This is due both to the lining up of the two single-well electron energy levels and to the Coulomb attraction of the hole. This continues with the increase of the field until, when $F \simeq 2.5$ kV/cm, it becomes energetically favorable for the hole to move into the second well. This change in hole location is enough to pull the electron, via the Coulomb attraction, back into the second well. At a slightly higher field of $F \simeq 5$ kV/cm, the potential due to the tilting of the wells overcomes the Coulomb attraction and the electron gradually moves into the first well. The effect of this oscillation on the oscillator strengths of the four states is seen in Fig. 16. Thus the effect of the Coulomb interaction is to considerably modify the dipole moment and to enhance the oscillator strength of the ground state for field strengths in the range -10 kV/cm $< F < 20$ kV/cm.

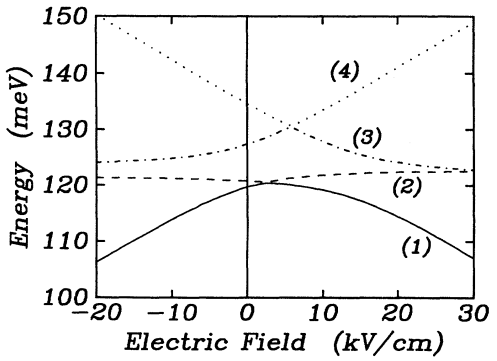

FIG. 14. The energy, relative to the band gap of GaAs, as a function of electric field for the four states of the novel Ga-Al-As structure with layer thicknesses $L_1 = 40$ Å, $L_2 = 55$ Å, and $L_b = 35$ Å. As can be seen, the ground state of the structure has a finite dipole moment even when $F = 0$. The number in parentheses beside each curve labels the quantum number of the state.

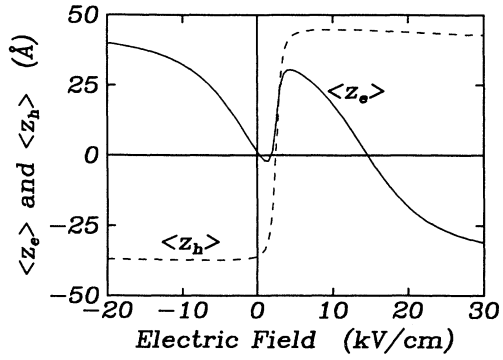

FIG. 15. The mean values $\langle z_e \rangle$ and $\langle z_h \rangle$ of the electron and hole positions in the growth direction as functions of the electric field for the *ground state* ($n = 1$) of the structure of Fig. 14.

VI. SUMMARY

We have developed a method of calculation of the exciton states in coupled-double-quantum-well structures in

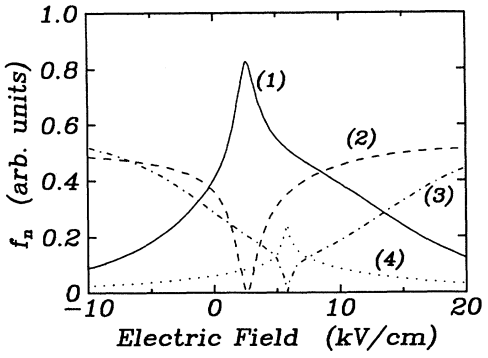

FIG. 16. The oscillator strength per unit area for the four exciton states for the same structure as in Fig. 14 as a function of the electric field. The number in parentheses beside each curve labels the quantum number of the state.

static electric fields that appears to be accurate for $GaAs/Ga_{1-x}Al_xAs$ structures with well widths, $L_i \lesssim a_0$, and barrier widths that are not so narrow that the single-particle tight-binding approximation breaks down ($L_b \gtrsim 15$ Å). We have demonstrated the importance of allowing for both coupling of the single-particle states and the differences in the radial behavior of the intrawell and interwell potions of the excitonic wave functions. From the comparison of our results with the results found using other types of wave functions, we feel that the most appropriate basis for exciton wave functions in multiwell structures is made up of *excitonic* wave functions rather than single-particle eigenstates. Finally, we have presented the results for a system that displays some very interesting excitonic behavior in the presence of a static electric field.

ACKNOWLEDGMENTS

This work was supported by the National Sciences and Engineering Research Council of Canada and the Ontario Laser and Lightwave Research Centre.

[1]Doyeol Ahn, IEEE J. Quantum Electron. **25**, 2260 (1989).
[2]Yasunori Tokuda, Kyozo Kanamoto, and Noriaki Tsukada, Appl. Phys. Lett. **56**, 166 (1990).
[3]D. A. B. Miller, J. S. Weiner, and D. S. Chemla, IEEE J. Quantum Electron. **QE-22**, 1816 (1986).
[4]S. Charbonneau, M. L. W. Thewalt, Emil S. Koteles, and B. Elman, Phys. Rev. B **38**, 6287 (1988).
[5]Y. J. Chen, Emil S. Koteles, B. S. Elman, and C. A. Armiento, Phys. Rev. B **36**, 4562 (1987).
[6]H. Q. Le, J. J. Zayhowski, and W. D. Goodhue, Appl. Phys. Lett. **50**, 1518 (1987).
[7]Y. Tokuda, K. Kanamoto, N. Tsukada, and T. Nakayama, Appl. Phys. Lett. **54**, 1232 (1989).
[8]Yasunori Tokuda, Kyozo Kanamoto, Yuji Abe, and Noriaki Tsukada, Phys. Rev. B **41**, 10 280 (1990).
[9]F. Clérot, B. Deveaud, A. Chomette, A. Regreny, and B. Sermage, Phys. Rev. B **41**, 5756 (1990).
[10]C. C. Phillips, R. Eccleston, and S. R. Andrews, Phys. Rev. B **40**, 9760 (1989).
[11]See, e.g., G. Bastard, E. E. Mendez, L. L. Chang, and L. Esaki, Phys. Rev. B **26**, 1974 (1982); R. L. Greene, K. K. Bajaj, and D. E. Phelps, *ibid.* **29**, 1807 (1984); J. A. Brum and G. Bastard, J. Phys. C **18**, L789 (1985).
[12]Tsuneo Kamizato and Mitsuru Matsuura, Phys. Rev. B **40**, 8378 (1989).
[13]Ian Glabraith and Geoffrey Duggan, Phys. Rev. B **40**, 5515 (1989).
[14]Johnson Lee, M. O. Vassell, Emil S. Koteles, and B. Elman, Phys. Rev. B **39**, 10 133 (1989).
[15]M. M. Dignam and J. E. Sipe, Phys. Rev. B **41**, 2865 (1990).
[16]A. Chomette, B. Lambert, B. Deveaud, F. Clérot, A. Regreny, and G. Bastard, Europhys. Lett. **4**, 461 (1987).
[17]G. Mo and C. C. Sung, Phys. Rev. B **38**, 1978 (1988).
[18]W. T. Masselink, P. J. Pearah, J. Klem, C. K. Peng, H. Morkoç, G. D. Sanders, and Yia-Chung Change, Phys. Rev. B **32**, 8027 (1985).
[19]Hanyou Chu and Yia-Chung Change, Phys. Rev. B **39**, 10 861 (1989).
[20]M. M. Dignam and J. E. Sipe, Phys. Rev. Lett. **64**, 1797 (1990).
[21]M. M. Dignam and J. E. Sipe, Phys. Rev. B (to be published).
[22]F. Agulló-Rueda, E. E. Mendez, and J. M. Hong, Phys. Rev. B **40**, 1357 (1989).
[23]E. E. Mendez, F. Agulló-Rueda, and J. M. Hong, Phys. Rev. Lett. **60**, 2426 (1988).
[24]G. D. Sanders and Yia-Chung Change, Phys. Rev. B **32**, 5517 (1985).
[25]Walter L. Bloss, J. Appl. Phys. **65**, 4789 (1989).
[26]D. Emin and C. F. Hart, Phys. Rev. B **36**, 7353 (1987).
[27]See, e.g., N. W. Ashcroft and N. D. Mermin, *Solid State Physics* (Holt, Rinehart, and Winston, Philadelphia, 1976), Chap. 8.
[28]E. J. Austin and M. Jaros, J. Phys. C **19**, 533 (1986).
[29]E. J. Austin and M. Jaros, Phys. Rev. B **31**, 5569 (1985).
[30]R. A. Smith, *Wave Mechanics of Crystalline Solids* (Chapman, London, 1969), Chap. 4.
[31]See, e.g., Walter Kauzmann, *Quantum Chemistry* (Academic, New York, 1967), Chap. 11.
[32]Walter L. Bloss, J. Appl. Phys. **67**, 1421 (1990).
[33]J. M. Luttinger and W. Kohn, Phys. Rev. **97**, 869 (1955).
[34]Alex Harwit and J. S. Harris, Jr., Appl. Phys. Lett. **50**, 685 (1987).